GEOPHYSICAL RESEARCH LETTERS, VOL. 33, L23303, doi:10.1029/2006GL027706, 2006

Impact of a priori zenith hydrostatic delay errors on GPS estimates of station heights and zenith total delays

P. Tregoning[1] and T. A. Herring[2]

Received 2 August 2006; revised 17 October 2006; accepted 24 October 2006; published 5 December 2006.

[1] Corrections to zenith atmospheric delays (including hydrostatic components) are estimated in geodetic analyses using partial derivatives that relate wet delays to the phase observations. At low-elevation angles, partial derivatives of the hydrostatic and wet delays are sufficiently different as to cause errors in the estimates of station heights and zenith total delays unless accurate surface pressure values are used to model the hydrostatic delay. The associated errors are latitude dependent because sites at high latitudes have a higher percentage of low-elevation observations. A priori zenith hydrostatic delay errors project into GPS height estimates with typical sensitivities of up to −0.2 mm/hPa, depending on the elevation angle cutoff and elevation angle dependent data weighting used in the analysis. This generates height errors of up to 10 mm and seasonal variations of up to 2 mm amplitude. The errors in zenith delay estimates are about half the magnitude of the height errors. **Citation:** Tregoning, P., and T. A. Herring (2006), Impact of a priori zenith hydrostatic delay errors on GPS estimates of station heights and zenith total delays, *Geophys. Res. Lett.*, *33*, L23303, doi:10.1029/2006GL027706.

1. Introduction

[2] Space geodetic techniques involve the observation of signals received from Earth-orbiting satellites and stellar bodies. Deformation of the Earth [e.g., *Blewitt et al.*, 2001] and changes in the Earth's gravity field [e.g., *Tapley et al.*, 2004] caused by mass redistribution have been detected using these techniques. However, limitations in geodetic analyses can cause systematic errors and spurious periodic variations in station heights [e.g., *Boehm et al.*, 2006; *Watson et al.*, 2006; *Stewart et al.*, 2005]. Comparisons between coordinate estimates from different techniques [e.g., *Ray and Altamimi*, 2005] are critical for defining a coherent terrestrial reference frame, while comparisons of atmospheric delays provide information on the absolute accuracy of each of the techniques [e.g., *Snajdrova et al.*, 2006].

[3] Modeling of the tropospheric retardation of the incoming signals remains a limiting factor on the accuracy of the analyses of Very Long Baseline Interferometry (VLBI), Satellite Laser Ranging (SLR) and Global Positioning System (GPS) observations. A common approach to treating the tropospheric delay effects in space-geodetic analyses is to model a priori the delay in the zenith (Zenith Total Delay, ZTD), relate the ZTD to the delay at any elevation angle through an empirical "mapping function" and to estimate discrete corrections to the a priori ZTD model to capture the time-varying nature of the atmosphere.

[4] The ZTD is generally broken into two separate parts: the zenith hydrostatic delay (ZHD) and the zenith wet delay (ZWD) caused by the presence of atmospheric water vapour. The hydrostatic delay can be modeled accurately from knowledge of the surface atmospheric pressure [e.g., *Saastamoinen*, 1972], whereas the wet delay changes temporally in an unpredictable manner. Both delays exhibit similar elevation angle dependence and only one parameter is used to estimate corrections for the combined effect of the hydrostatic and wet delays.

2. Modeling the Tropospheric Delay

[5] The ZHD can be modeled as [*Saastamoinen*, 1972]:

$$ZHD = \frac{0.00227768 P_0}{1 - 0.00266\cos(2\phi) - 0.00028 h_{ref}} \quad (1)$$

where P_0 is the surface pressure at the site, ϕ is the site latitude and h_{ref} is the site height (in km) above the geoid. The slant total delay (STD) at elevation angle ϵ is:

$$STD(\epsilon) = mf_h(\epsilon) ZHD + mf_w(\epsilon) ZWD \quad (2)$$

where mf_h is the hydrostatic mapping function and mf_w is the wet mapping function.

[6] In typical VLBI and GPS analyses, the ZTD is parameterised as either a step or piecewise linear function with parameters estimated at time intervals varying from 30 minutes to 4 hours or as a stochastic process [e.g., *Emardson et al.*, 1998]. The partial derivative used to relate the ZTD parameters to the observed phase, $\partial ZTD/\partial\phi$, is usually the wet mapping function, $mf_w(\epsilon)$ (see Equation 2). Any adjustment required to the a priori value of ZHD is also estimated as part of the corrections to ZWD. Other approaches could be used such as the Total Mapping Function [*Boehm et al.*, 2006] or estimating corrections to both the ZHD and ZWD; no studies have been reported where GPS data have been analysed with these approaches.

[7] Two physical effects are typically estimated with only one parameter in the modeling and parameterisation of the hydrostatic and wet gradients. Some investigations have been made using VLBI data in which the hydrostatic gradients are modeled then corrections estimated for the wet gradients [e.g., *Niell*, 2003]; we focus in this paper on ZHD alone and leave the discussion of gradients in GPS analyses for future study.

[1] Research School of Earth Sciences, Australian National University, Canberra, ACT, Australia.
[2] Department of Earth, Atmospheric and Planetary Sciences, Massachusetts Institute of Technology, Cambridge, Massachusetts, USA.

0094-8276/06/2006GL027706$05.00

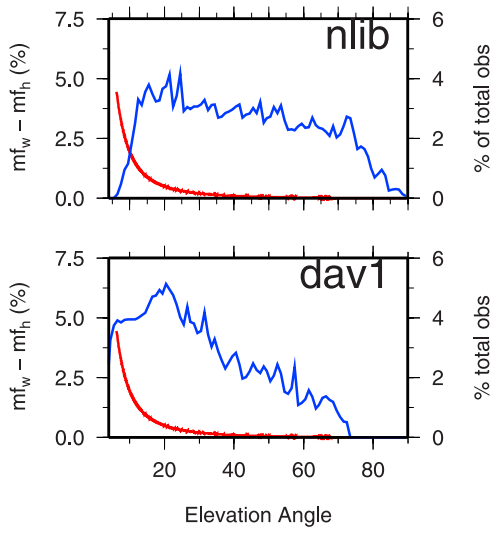

Figure 1. Difference between hydrostatic and wet mapping functions (expressed as a percentage of the hydrostatic mapping function) for the Niell Mapping Functions (red) at high latitude site (Davis, 67°S) and mid-latitude site (North Liberty, 41°N). The percentage of observations at each elevation angle (1° bins) for a typical 24 hour period is shown in blue. 24% and 8% of the observations occur below 15° elevation for Davis and North Liberty, respectively.

[8] *Boehm et al.* [2006] showed from a reduction of variance study that VLBI baseline statistics degrade when a static pressure value is used to model a priori the ZHD, akin to the common practice in most GPS analyses today. The important consideration is whether the hydrostatic delay partial derivative is sufficiently different from the wet delay partial derivative (that is actually used to estimate corrections to the ZHD) as to introduce errors into the ZTD corrections. Figure 1 shows the differences in hydrostatic and wet mapping functions of *Niell* [1996] at two different sites, expressed as a percentage of the hydrostatic mapping functions. The errors in the partial derivatives are dependent on the observation geometry and, in general, the differences between the hydrostatic and wet components range from <0.5% at 20° to nearly 5% at 5° elevation angle.

3. Atmospheric Pressure for Calculating A Priori ZHD

[9] In GPS analyses the surface pressure used in Equation 1 is generally derived using a "standard (constant) atmospheric value" at sea level (hereafter called 'standard sea level' (SSL)) which is then corrected for the station height above sea level [*Hopfield*, 1969]:

$$P_0 = P_{sl}\left(\frac{T_k - \alpha h_{ref}}{T_k}\right)^{(g/R\alpha)} \quad (3)$$

where P_{sl} is the atmospheric pressure at sea level (assumed to be 1013.25 hPa), T_k is the atmospheric temperature at sea level in kelvin (assumed to be 293.16°K), α is the normal lapse rate of temperature with elevation (e.g., 4.5 K/km as used in the GAMIT software [*King and Bock*, 2006]), g is gravity at the surface of the Earth (9.7867 m/s^2) and R is the gas constant (0.287 kJ/°/kg for dry air). Values for surface pressure could also be derived from actual surface observations, global pressure fields (e.g., European Center for Medium Range Weather Forecasting (ECMWF)) or from the Global Pressure and Temperature model (GPT) (J. Boehm et al., Global Pressure and Temperature (GPT): A spherical harmonic expansion of annual pressure and temperature variations for geodetic applications, submitted to *Journal of Geodesy*, 2006), derived from a spherical harmonic representation of monthly mean surface pressure (Sep'99 to Aug'02) from the ECMWF ERA40 numerical weather model.

[10] Figure 2 shows the error in SSL pressure, assuming that the GPT model is the "true" mean surface pressure.

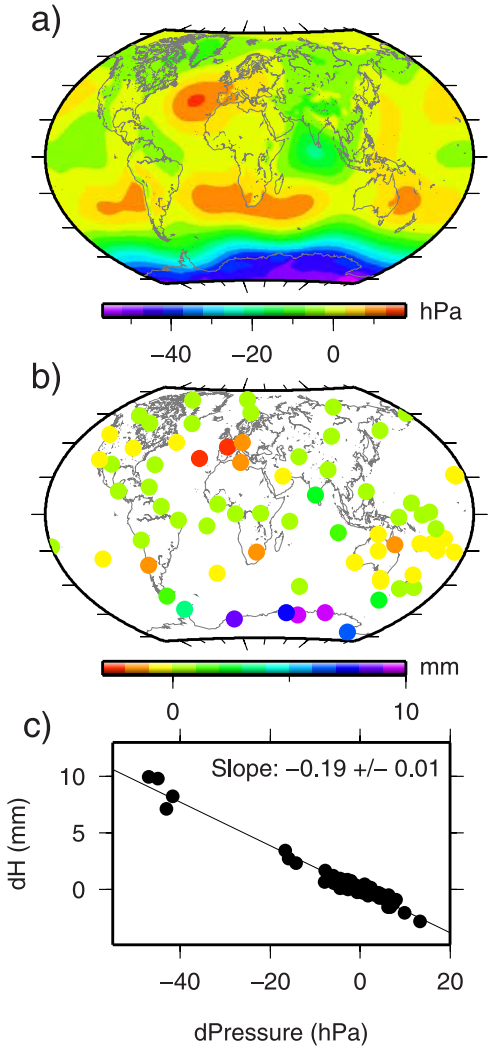

Figure 2. (a) Error in surface pressure derived from "standard" sea level pressure with respect to the mean surface pressure derived from the GPT model (i.e., GPT-SSL). (b) Error in station height estimates caused by using SSL a priori pressure. (c) Relation between a priori pressure errors and height differences. Elevation-dependent weighting was used in the GPS analysis with a minimum elevation angle of 7°.

There is a clear spatially varying pattern, with a maximum error of −56 hPa (in Antarctica) and a global RMS of 7 hPa. A geographically coherent negative bias is found at high southern latitudes that is reflected in changes in station height estimates when a priori pressure from the GPT model is used in place of SSL (Figure 2b, see Section 5 for a description of the height estimation from GPS data). There is a sensitivity of −0.19 mm height change for every 1 hPa error in a priori surface pressure (Figure 2c).

[11] The effect of a +10 hPa change in the a priori surface pressure, P_0, in Equation 1 is a +22.8 mm change in a priori ZHD. Mapped to 10° elevation, this amounts to a change in a priori slant delay of +126.2 mm. Therefore, extreme differences in actual and SSL pressure seen at sites such as Davis, Antarctica (e.g., 60 hPa on day 220 of 2005) represent slant range a priori modeling errors of over 0.7 m at 10° and approximately 15 mm difference between the hydrostatic and wet mapping functions.

[12] Annual fluctuations in surface pressure vary geographically with amplitudes from 0 to ∼10 hPa (not shown). Such periodic variations would alias into periodic variations in station heights and ZTD estimates if constant a priori pressure is used. For example, the strong annual variations seen in atmospheric pressure observed at Bahrain (amplitude of ∼9 hPa) would create an annual variation in height with an amplitude of ∼1.7 mm.

4. Simulations

[13] We developed a simple simulator, equivalent to precise-point-positioning, to study this problem. We used 24-hour sessions estimating station position, atmospheric delays and phase ambiguities (solutions with ambiguities resolved to integers as well as solutions with ambiguities left as real values). Elevation cutoff angles and elevation angle data weighting of the form $\sigma^2 = a^2 + (b/\sin(\epsilon))^2$ were implemented. The model error driving the simulator is the difference between the Niell hydrostatic and wet mapping functions at 60°S, scaled by the effect of a +100 hPa error in the surface pressure. Neither the stochastic treatment of atmospheric delay estimation nor ambiguity resolution greatly affected the sensitivity of the height estimates and average ZTDs to errors in modeling the ZHD, whereas elevation cutoff angle and elevation angle dependent data weighting affected both height and ZTD estimates. Latitude and, to a small degree, longitude affected mainly the height sensitivity but not the ZTD sensitivity. Comparison of the simulation results with those from real-data analysis in point position mode showed good agreement in both height and ZTD sensitivity (the differences arose from data distribution differences due to signal acquisition and editing). Comparison of results with network processed GPS results (for a 40-station global network) showed good agreement for the height sensitivity but the network solution showed ZTD sensitivity 80% larger than the simulations. This probably results from the fact that simulated data include all possible observations whereas in real data low-elevation angle observations are sometimes not acquired or are edited out (multipath/turbulent atmospheric effects). Sensitivities between −0.12 and −0.19 mm/hPa occur in station heights and 0.055–0.065 mm/hPa in ZTD. For a 10° elevation angle cutoff with no elevation angle dependent data weighting, the sensitivity of height estimates to errors in the surface pressure, averaged over all latitudes, was −0.139 mm/hPa for both the simulation and network solutions. The sensitivity of the average ZTD estimate was 0.058 mm/hPa from the simulations and 0.076 mm/hPa from the network solution.

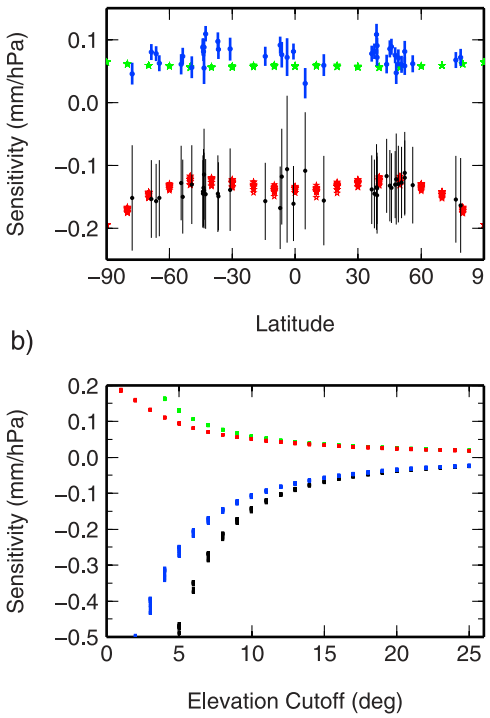

Figure 3. (a) Height (red: simulated; black: estimated, with 1σ error bars) and ZTD (green: simulated; blue: estimated, with 1σ error bars) errors versus latitude as a function of error in surface pressure used to calculate the a priori ZHD (+100 hPa for simulations, difference between SSL and actual pressure for estimated network solutions). Uniform 10 mm data weighting and 10° cutoff angle applied. (b) Height (black/blue) and ZTD (red/green) errors at Davis, Antarctica, for different elevation cutoff angles as a function of error in surface pressure used to calculate the a priori ZHD. Simulated values throughout the year are shown assuming a static GPS constellation. Elevation-dependent weighting of $a^2 + (b/\sin(\epsilon))^2$ (blue and red results) and constant data weighting (black and green) were used.

[14] Figure 3a shows the errors in simulated station heights and ZTDs as a function of station latitude. The station height errors are clearly related to the latitude of the stations, with the pattern being symmetric about the equator when averaged over longitude.

[15] Given that the differences in the partial derivatives of relating the hydrostatic or wet delays to the phase observations are greater for observations at lower elevation angles, the higher percentage of low-elevation observations seen at high latitude sites amplifies the effect of an a priori ZHD error. Varying the minimum elevation angle used in the analysis and including lower elevation observations increases the errors in station heights and ZTD (Figure 3b). The horizontal coordinates can also be affected but the

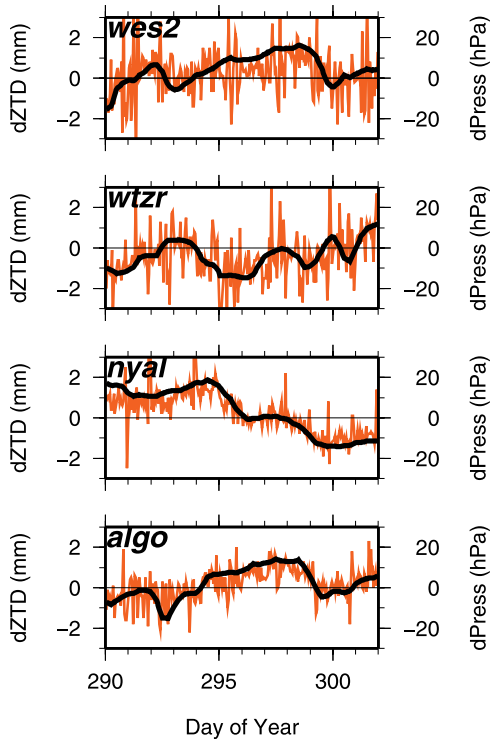

Figure 4. Differences in GPS estimates of ZTD at Algonquin, Ny Alessund, Wettzell and Westford computed using static or observed surface pressure to derive the a priori ZHD. The difference in the surface pressure is shown in black. Typical values of elevation-dependent weighting are $9^2 + (5/\sin(\epsilon))^2$ mm^2.

errors are <0.4 mm for a 100 hPa pressure error. Similar patterns are obtained from height and ZTD estimates using real data, although the latitudinal symmetry is less evident.

5. Analyses of Actual GPS Observations

[16] We analysed GPS data using the GAMIT software with a double-difference approach, estimating station coordinates, satellite orbits, earth orientation parameters and ZTD corrections as a piecewise linear model with nodes every hour. Non-tidal atmospheric pressure loading was applied [*Tregoning and van Dam*, 2005] and we used the VMF1 mapping function [*Boehm et al.*, 2006]. We generated daily solutions for a global network of ~75 sites during 2004 using elevation-dependent weighting of observations and an elevation cutoff angle of 7°.

[17] Three sets of solutions were generated, differing only in the source of atmospheric pressure used to model the a priori ZHD: a) static SSL, b) surface pressure derived from the GPT model and c) either observed surface pressure at the GPS sites or values derived from the GPT model if no meteorological observations were available. There is a high correlation between differences in the ZTD estimates from different solutions and changes in surface pressure used to compute the a priori ZHD (Figure 4) and the magnitudes are compatible with the differences predicted from our simulations. Furthermore, differences in actual mean station height estimates can be up to 10 mm (see, for example, the Antarctic sites in Figure 2b), again reflecting the effects seen in the simulations. The pattern of height biases correlates spatially with the errors in a priori pressure (as shown in Figure 2 from the error in SSL pressure with respect to GPT pressure).

[18] We now look in detail at one specific period in the time series of site Rio Grande, Argentina. During days 312–317, the observed surface pressure increased by over 30 hPa, then subsequently decreased back to 'average' values (Figure 5). The station height estimates from the solutions with constant surface pressure values vary during this period by ~6 mm, consistent with the ~−0.19 mm/hPa relation between height and a priori pressure error. The height estimates when surface pressure observations (10 minute sampling) were used a priori to model the ZHD do not show the same corresponding variation. Thus, height errors caused by high frequency pressure variations (not modeled by the GPT or a static value) can be mitigated by using observed surface pressure data. The height errors and atmospheric pressure loading deformation have opposite signs (see day 315 in Figure 5); therefore, they interfere destructively in analyses that do not account properly for either effect.

6. Conclusions

[19] Not using accurate surface pressure leads to errors in the a priori ZHD values which, in turn, corrupt the estimates of station heights and ZTD values in GPS analyses. Depending on the temporal variations of the differences between actual surface pressure and the typically assumed static value, this can lead to height biases of −0.1 to −0.2 mm/hPa and possibly even annual variations with amplitudes of up to 2 mm. Deformation caused by atmospheric pressure loading is around 0.4–0.5 mm/hPa for inland sites; therefore, geodetic analyses that do not model atmospheric pressure loading and use static a priori pressure for modeling the ZHD will underestimate the elastic deformation by ~20%. If the results of the analysis of GPS observations are to be assimilated with other space-geodetic results (e.g., in formulating ITRF products) then it is imperative that a more accurate approach be adopted for modeling the a priori ZHD. Using temporally varying

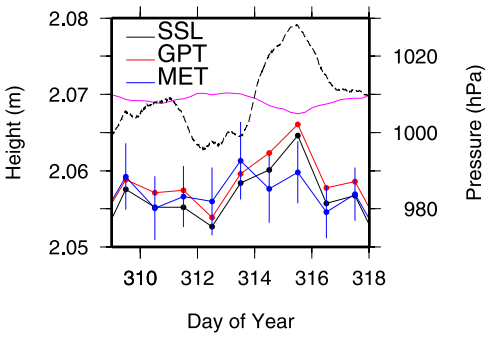

Figure 5. Station height estimates for RIOG using pressure from static SSL, GPT and actual observations (MET). 1σ formal error bars are shown on the height estimates for the MET solutions. The observed surface pressure is shown as a dashed black line while the atmospheric pressure loading deformation (corrected for in the GPS analyses) is shown in pink, offset by 2.07 m.

values of surface pressure - or even using a priori estimates of ZHD as derived from a numerical weather model [e.g., *Boehm et al.*, 2006] - will make the approach of GPS analysis more compatible with other space-geodetic techniques.

[20] GPS coordinate estimates will (indeed 'should') never agree with VLBI/SLR estimates unless the "standard" approach of modeling a priori the ZHD in the analysis of GPS data is replaced by something more accurate. The GPT model for a priori atmospheric pressure removes the majority of the mean height biases caused by using a static pressure value. However, only using observed surface pressure permits the high-frequency variations in ZHD to be modeled properly, thus preventing the propagation of these variations into station height and ZTD estimates.

[21] **Acknowledgments.** We thank the IGS for making global GPS and meteorological data available, J. Boehm for helping to integrate the VMF1 and the GPT models into the GPS analysis and two anonymous reviewers for their comments. Bob King made many helpful suggestions during this study. This work was partly supported by NASA grant NAS5-99007. Figures plotted with the GMT software [*Wessel and Smith*, 1998].

References

Blewitt, G., D. Lavallee, P. Clarke, and K. Nurutdinov (2001), A new global mode of Earth deformation: Seasonal cycle detected, *Science*, *294*, 2342–2345.

Boehm, J., B. Werl, and H. Schuh (2006), Troposphere mapping functions for GPS and very long baseline interferometry from European Centre for Medium-Range Weather Forecasts operational analysis data, *J. Geophys. Res.*, *111*, B02406, doi:10.1029/2005JB003629.

Emardson, T. R., G. Elgered, and J. M. Johansson (1998), Three months of continuous monitoring of atmospheric water vapor with a network of Global Positioning System receivers, *J. Geophys. Res.*, *103*, 1807–1820.

Hopfield, H. S. (1969), Two-quartic tropospheric refractivity profile for correcting satellite data, *J. Geophys. Res.*, *74*, 4487–4499.

King, R. W., and Y. Bock (2006), Documentation for the GAMIT GPS processing software, release 10.2, report, Mass. Inst. of Technol., Cambridge.

Niell, A. E. (1996), Global mapping functions for the atmosphere delay at radio wavelengths, *J. Geophys. Res.*, *101*, 3227–3246.

Niell, A. E. (2003), The IMF Mapping functions—REV.2, paper presented at GPSMet Workshop, Intl. Union of Geodesy and Geophys., Tsukuba, Japan.

Ray, J., and Z. Altamimi (2005), Evaluation of co-location ties relating the VLBI and GPS reference frames, *J. Geod.*, *79*, 189–195.

Saastamoinen, J. (1972), Atmospheric correction for the troposphere and stratosphere in radio ranging of satellites, in *The Use of Artificial Satellites for Geodesy*, *Geophys. Monogr.*, vol. 15, edited by S. W. Henriksen et al., pp. 247–251, AGU, Washington, D. C.

Snajdrova, K., J. Boehm, P. Willis, R. Haas, and H. Schuh (2006), Multitechnique comparison of tropospheric zenith delays derived during the CONT02 campaign, *J. Geod.*, *79*, 613–623.

Stewart, M. P., N. T. Penna, and D. D. Lichti (2005), Investigating the propagation mechanism of unmodelled systematic errors on coordinate time series estimated using least squares, *J. Geod.*, *79*, 479–489.

Tapley, B. D., S. Bettadpur, M. Watkins, and C. Reigber (2004), Grace recovery and climate experiment: Mission overview and early results, *Geophys. Res. Lett.*, *31*, L09607, doi:10.1029/2004GL019920.

Tregoning, P., and T. van Dam (2005), Atmospheric pressure loading corrections applied to GPS data at the observation level, *Geophys. Res. Lett.*, *32*, L22310, doi:10.1029/2005GL024104.

Watson, C., P. Tregoning, and R. Coleman (2006), Impact of solid Earth tide models on GPS coordinate and tropospheric time series, *Geophys. Res. Lett.*, *33*, L08306, doi:10.1029/2005GL025538.

Wessel, P., and W. H. F. Smith (1998), New, improved version of the Generic Mapping Tools released, *Eos Trans. AGU*, *79*, 579.

T. A. Herring, Department of Earth, Atmospheric and Planetary Sciences, Massachusetts Institute of Technology, Cambridge, MA 02139, USA. (tom.herring@mit.edu)

P. Tregoning, Research School of Earth Sciences, Australian National University, Mills Road, Canberra, ACT 0200, Australia. (paul.tregoning@anu.edu.au)